ACS Catalysis

Research Article

pubs.acs.org/acscatalysis

Mo−Ni/Al-SBA-15 (Sulfide) Catalysts for Hydrodenitrogenation: Effect of Si/Al Ratio on Catalytic Activity

C. Suresh,[†] D. Santhanaraj,[†] M. Gurulakshmi,[†] G. Deepa,[†] M. Selvaraj,[†] N. R. Sasi Rekha,[‡] and K. Shanthi*,[†]

[†]Department of Chemistry, Anna University, Chennai 600025, India

[‡]Department of Chemistry, Anna University of Technology, Tiruchirappalli 620024, India

ABSTRACT: Mesoporous Al-SBA-15 with different Si/Al molar ratio (10, 20, 30, and 40) was synthesized hydrothermally, and Mo−Ni catalysts were prepared by incipient wet impregnation method and characterized by different techniques. An impressive catalytic performance was observed on Mo−Ni/Al-SBA-15(10) for Methylcyclohexylamine conversion to hydrocarbons. The observed trend of activity is correlated with the aluminum content, and it is concluded that the variation in Si/Al ratio remarkably affects the hydrodenitrogenation ability of Al-SBA-15 supported Mo−Ni catalysts.

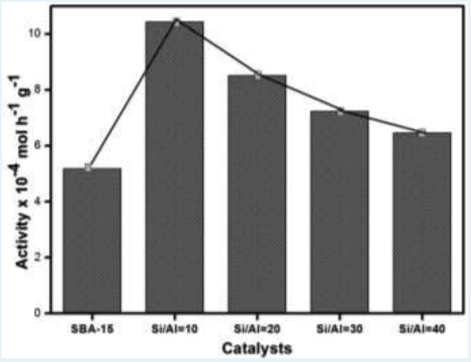

KEYWORDS: *hydrodenitrogenation, methylcyclohexylamine, SBA-15, Al-SBA-15, Mo−Ni catalysts*

1. INTRODUCTION

The industrial application of hydrotreating catalysts lies in the wealth of processes applied to upgrade and process crude oil to comply with current technological and environmental standards. Hydrotreating processes are reductive hydrogen treatments of the organic molecules comprising crude oil, to remove heteroatoms like nitrogen, oxygen or sulfur.[1] The purpose of removing such impurities is 2-fold. The burning of S and N containing fuels presents a severe threat to the environment, that is, the formation of acid rain from SO_2 or NO_x emissions. Additionally, other transition-metal based catalysts treating the crude oil fractions generally have a very low tolerance against impurity atoms like S, and if untreated, the sulfur leads to an accelerated deactivation and breakdown of the catalyst. The type of catalysts used for hydrotreating processes is mainly dependent on the specific reaction and process requirements. In general, catalysts for hydrotreating reactions consist of mixed sulfides of CoMo, NiMo, or NiW supported on high surface area carriers like γ-Al_2O_3. In recent times, many efforts are aimed to improve the catalytic activity of hydrotreating catalysts by using new materials as catalytic support.

There are many approaches to prepare better catalysts to meet these challenges, like changing the active component, varying the preparation method, and changing the support or permutations and combinations of these. In recent years, there has been a keen interest in new supports for the hydrotreating catalysts because of the need to develop better catalysts and the availability of large number of new materials of high surface area that may be suitable for support application, as well as the initial success in increasing the activity by using novel supports. For a support to see commercial applications it is not enough to have suitable chemical characteristics; it should also have proper physical and mechanical properties to withstand the rigors of high-pressure operation and regeneration in commercial reactors. The effect of the support on catalytic actions is an intriguing topic.[2] The alteration of catalytic activities because of the support may arise as a result of important factors like variation in dispersion and morphology of the active component and possible metal support interactions. Support can also influence the reactivity by favoring exposure of some crystallographic planes in preference to other by edge bonding or basal plane bonding of the sulfided phase. Morphological changes and metal support interactions show that the support may change the activity and/or selectivity of the catalysts. Understanding support effects in hydrotreating is intimately connected with other areas of hydrotreating related research, such as structure of the catalyst and origin of catalytic functionalities. Support has an indirect role in determining the promotional effect by altering the number of promoted atoms that can be accommodated at the edges and the energetics of the site with which promoter is associated.

A group of mesoporous molecular sieves MCM-41 type materials containing high surface area (700−1000 m^2/g) and 20−35 Å pore diameter attracted much interest in the hydrotreating process,[3,4] but the poor hydrothermal stability

Received: July 27, 2011
Revised: November 28, 2011
Published: December 13, 2011

   dx.doi.org/10.1021/cs200385y | *ACS Catal.* 2012, 2, 127−134

of these materials represents a serious limitation to their practical application. Hence, a novel family of mesoporous silicate (SBA-15) with larger pores, thicker pore walls, and high hydrothermal stability has attracted attention recently as a support for hydrotreating reaction. Vradman and Sampieri et al.[5,6] studied the hydrodesulphurization reaction over NiMo supported SBA-15 catalysts and found that SBA-15 supported catalysts show superior activity compared to the conventional γ-Al_2O_3 supported catalysts. It was also found that aluminum or titanium incorporation in the SBA-15 materials provide better dispersion of nickel and molybdenum species.[7] Sundaramurthy et al.[8] studied the hydrotreating activity of siliceous, boron and aluminum substituted SBA-15 toward hydrotreating of gas oil and reported that the incorporation of heteroatom into the silica matrix increases the hydrotreating property of the catalysts. Muthu Kumaran et al.[9] reported the effect of Si/Al ratio of Al-SBA-15 support on the behavior of Mo, CoMo, and NiMo catalysts for thiophene hydrodesulphurization and hydrogenation of cyclohexene and found that increase in Al content increases the molybdenum dispersion and anion vacancies leading to increase of HDS and HYD rates. Rota et al.[10,11] studied the role of partial pressure of H_2S on reaction pathway of methylcyclohexylamine hydrodenitrogenation. The conversion of MCHA was reported to be higher on Alumina-Silica-Alumina (ASA) supported catalyst than Al_2O_3 supported catalyst because of the fine dispersion of active metals and promoter in ASA than alumina.[12] However, a systematic study of variation of Si/Al ratio in the synthesis of Al-SBA-15 and its effect on the activity of mesoporous Al-SBA-15 supported Ni–Mo for methylcyclohexylamine hydrodenitrogenation has not been explored. In this article we report a detailed systematic study of hydrodenitrogenation functionalities of sulfided Mo–Ni supported on Al-SBA-15 with various Si/Al ratios and the physicochemical properties of oxidic form of the catalysts.

2. EXPERIMENTAL SECTION

2.1. Preparation and Characterization of the Support and Catalysts. The siliceous SBA-15 material was synthesized using Pluronic P123 ($EO_{20}PO_{70}EO_{20}$), Aldrich, (M_w = 5800) as the structure directing agent and tetraethyl orthosilicate (TEOS) as the silica source, following the procedure reported previously.[13] In a typical synthesis, 12 g of Pluronic P123 was dispersed in a calculated amount of distilled water, and the resultant solution is mixed with 2 M HCl at 40 °C. Then 25.5 g of TEOS was added to the above solution. The mixture was stirred at 40 °C for 24 h and then aged at 100 °C for 48 h without stirring. The obtained solid product was recovered by filtration, washed with deionized water and dried at 80 °C overnight. Calcination was carried out in static air at 550 °C for 6 h. This SBA-15 silica was used as a parent material to produce aluminum containing SBA-15 via postsynthetic grafting of aluminum.[14] In the preparation of aluminum containing SBA-15 material with different Si/Al ratio, the siliceous SBA-15 material was treated with aluminum isopropoxide dissolved in isopropanol; the obtained product was filtered and washed with isopropanol, dried, and calcined at 500 °C for 5 h. Mo–Ni impregnated catalysts were prepared by incipient wetness sequential impregnation method. In our previous study on AlMCM-41 supported catalysts[15] it is reported that the order of impregnation of the active components is an important factor in designing the supported catalyst and found that the impregnation of NiO first followed by MoO_3 gives an efficient catalyst. Hence, in the present investigation the catalysts were synthesized by impregnating 3% NiO followed by 12% MoO_3 using an appropriate concentration of nickel nitrate and ammonium heptamolybdate on Al-SBA-15 and represented as Mo–Ni/Al-SBA-15(x) where x represents the Si/Al ratio (10 to 40). After each impregnation the catalyst was dried in air at 100 °C overnight and calcined at 500 °C for 5 h.

The support and catalysts were characterized by X-ray diffraction (XRD), N_2 adsorption–desorption Brunauer–Emmett–Teller (BET) analysis, inductively coupled plasma optical emission spectroscopy (ICP-OES), diffuse reflectance spectroscopy (DRS), temperature programmed reduction (TPR), and ^{27}Al MAS NMR spectroscopic techniques in the oxidic form. The XRD pattern was recorded on a BRUCKER D8 diffractometer using Cu K_α radiation (λ = 1.54 Å) at a scan rate of 0.04° min^{-1} over the 2θ range of 0.5–60°. N_2 adsorption–desorption isotherms were measured with a BEL SORP mini II analyzer at liquid N_2 temperature. Prior to the experiments, the samples were degassed at 300 °C for 6 h. Surface area was calculated by the BET method (S_{BET}), the pore volume (V_P) was determined by nitrogen adsorption at a relative pressure of 0.98, and pore size distributions were determined from the desorption isotherms by using the Barrett–Joyner–Halenda (BJH) method. ICP-OES measurements were performed with a Perkin-Elmer OPTIMA 3000. DRS of powdered samples were recorded on a Shimadzu UV-2450 spectrophotometer over the range of 190–800 nm using barium sulfate as reference. TPR experiments were performed on a Micromeritics instrument equipped with a thermal conductivity detector. About 75 mg of the sample was pretreated at 115 °C in high pure helium gas atmosphere (25 cc/min) for 1 h and then cooled to room temperature in a helium atmosphere. Prior to the analysis the baseline correction was set to stable at room temperature using 5% H_2/Ar (25 cc/min), and TPR profiles were recorded from room temperature to 850 °C at a heating rate of 10 °C/min. Solid state ^{27}Al MAS NMR spectra were recorded on a BRUKER DSX 300, NMR Spectrometer with a magnetic field strength of 7.04 T; the ^{27}Al chemical shift was referenced using $Al(H_2O)_6^{3+}$.

2.2. Catalytic Activity. The catalytic activity of Mo–Ni(S)/Al-SBA-15 catalysts was evaluated for hydrodenitrogenation of methylcyclohexylamine (1:30 mol ratio of MCHA:-Tetralin) in a fixed bed flow reactor in presence of ultra pure hydrogen (50 cm^3/min) at atmospheric pressure. Methylcyclohexylamine has been chosen as a model compound for the present study as it is formed as an intermediate during the hydrodenitrogenation of parent heterocyclic nitrogen containing compounds present in the crude petroleum. Prior to the reaction the catalysts were sulfided in the flow of ditertiary butyl polysulfide (DBPS) and hydrogen (1:20 mmol of DBPS:H_2) at 400 °C for 3 h. The stability of the catalysts was tested for a period of 1 to 20 h at 350 °C. The gaseous product (ammonia) formed during the reaction was estimated by titration with 0.01 N hydrochloric acid,[16] and the liquid product (methylcyclohexane) was identified with GC-17A Shimadzu gas chromatograph instrument using a DB-5 silica fused column and thermal conductivity detector. The efficiency of the catalyst is expressed in terms of activity as mol h^{-1} g^{-1} using the equation, Activity = [(Amine feed (mol h^{-1}) × % Ammonia formed)/(Weight of the catalyst (g) × 100)]. The experiments were repeated at least three times for reproducibility. After every catalytic run the catalyst was regenerated by passing CO_2 free air over the catalyst at 500 °C for 6 h.

dx.doi.org/10.1021/cs200385y | ACS Catal. 2012, 2, 127–134

3. RESULTS AND DISCUSSION

3.1. XRD Analysis. The mesoporosity and crystalline nature of the SBA-15 and Al-SBA-15 materials with varying Si/Al ratio were confirmed by the low angle XRD technique (Figure 1); the XRD pattern shows the characteristic nature of

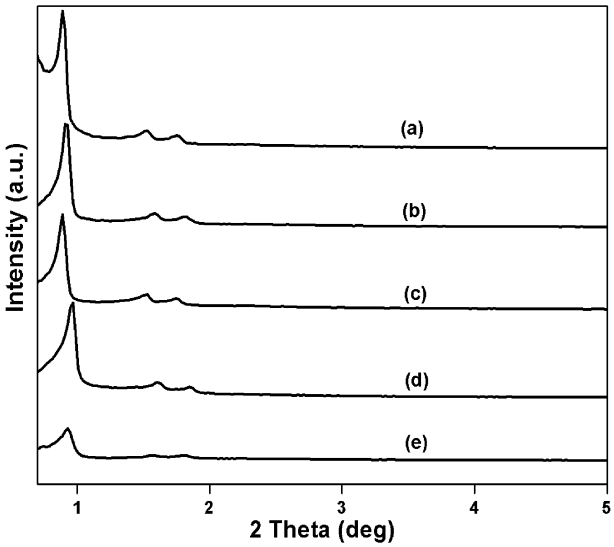

Figure 1. Low angle XRD patterns of support (a) Siliceous SBA-15, (b) Al-SBA-15 (10), (c) Al-SBA-15(20), (d) Al-SBA-15(30), and (e) Al-SBA-15(40).

mesoporous SBA-15.[13] The intense peak at 2θ = 0.9 and two small peaks in the range 2θ = 1.5−2 correspond to the (100), (110), and (200) diffraction planes, respectively. A small reduction in the peak intensities of aluminum incorporated samples was observed in comparison with siliceous SBA-15. Even though the incorporation of aluminum into silica framework slightly affects the structural properties of parent material, the hexagonal structure is retained. The low angle XRD patterns of Mo−Ni/Al-SBA-15 catalysts shown in Figure 2 confirm the mesoporous nature of SBA-15. The dispersion of the active metal and promoter on the Al-SBA-15 is very well understood from the high angle XRD patterns of Mo−Ni/Al-SBA-15 catalysts shown in Figure 3. Figure 3e, corresponding to the catalyst Mo−Ni/Al-SBA-15(10), did not show any crystalline molybdenum or nickel phase. This may be a strong indication of the finely dispersed nickel and molybdenum oxides over the surface of support. The fine dispersion of molybdenum oxide species by the incorporation of aluminum was also clearly explained by Olivas and Zepeda.[17] However, at low aluminum level, interaction of extra framework aluminum with Mo may decrease the dispersion of Mo and leads to the formation of bulk crystalline molybdenum oxide on the surface of the support. This is evidenced from the increasing peak intensity corresponding to the crystalline MoO_3 phase (Figure 3a and b).

3.2. Surface Area Analysis. N_2 adsorption−desorption isotherms of siliceous SBA-15 and Al-SBA-15(x) (x = 10, 20, 30, and 40) display a typical type-IV isotherm with two sharp inflections in the relative pressure range of 0.6−0.8 and H1-type hysteresis loop confirming the ordered nature of the mesoporous Al-SBA-15 (Figure 4). The capillary condensation between the two inflections indicates the presence of uniform mesopore channels; the pore size and BET surface area of

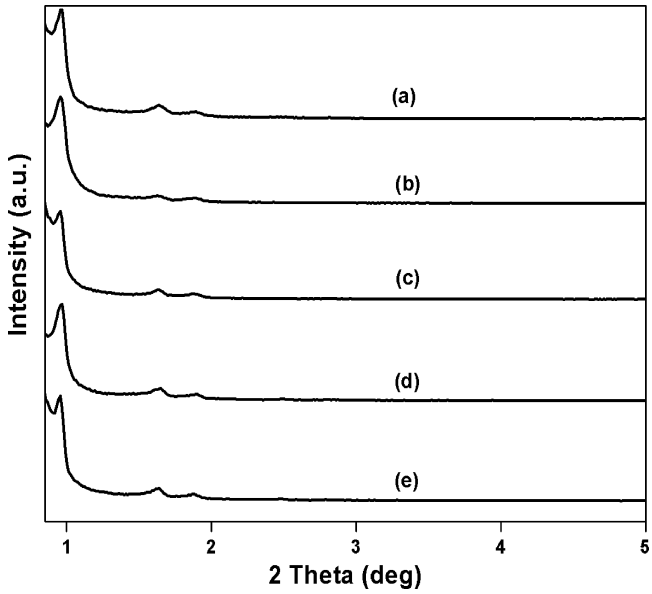

Figure 2. Low angle XRD patterns of Mo−Ni/Al-SBA-15 catalysts: (a) Siliceous SBA-15, (b) Al-SBA-15(10), (c) Al-SBA-15(20), (d) Al-SBA-15(30), and (e) Al-SBA-15(40).

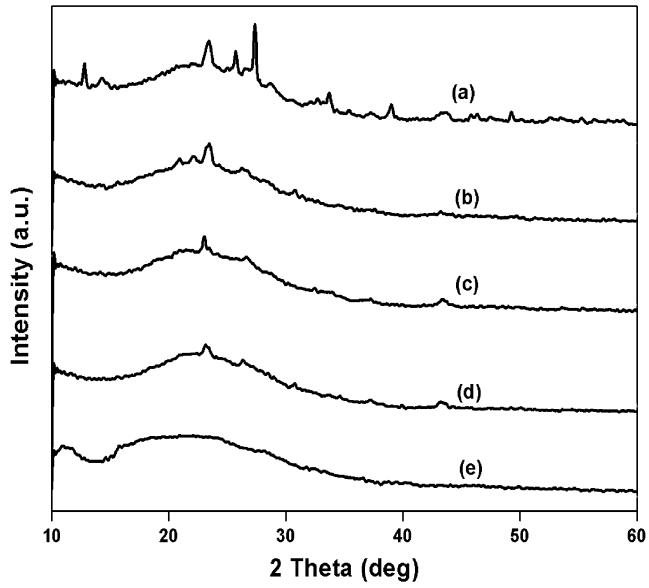

Figure 3. High angle XRD patterns of Mo−Ni/Al-SBA-15 catalysts: (a) SBA-15, (b) Al-SBA-15(40), (c) Al-SBA-15(30), (d) Al-SBA-15(20), and (e) Al-SBA-15(10).

siliceous SBA-15 and Al-SBA-15(x) support and Mo−Ni/Al-SBA-15(x) catalysts are shown in Table 1. After the introduction of aluminum, the type-IV isotherm with an H1-type hysteresis loop and narrow pore size distribution are still observed. However, a decrease in the value of surface area, pore volume, and pore size was observed with decreasing Si/Al ratio value of the catalysts synthesized by the post synthetic alumination procedure. This is in accordance with the literature report.[18] A further decrease only in the surface area and pore volume was observed on the impregnation of Mo and Ni over the support. However, the shape of the hysteresis loop was maintained even after the impregnation of active and promoter metals (Figure 4B). This confirms the retention of the

dx.doi.org/10.1021/cs200385y | ACS Catal. 2012, 2, 127−134

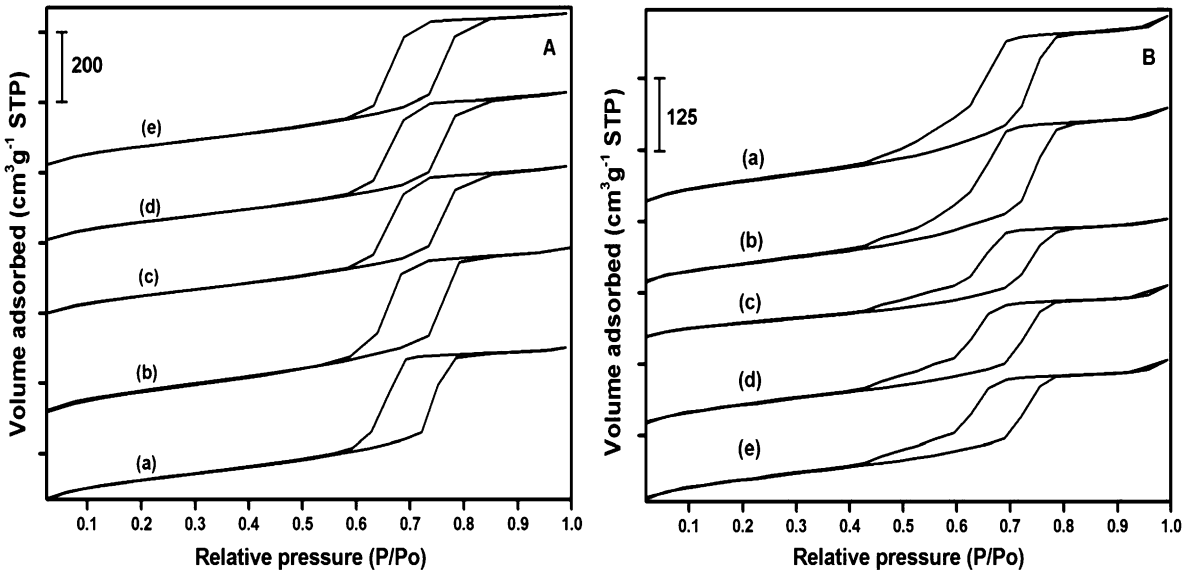

Figure 4. Nitrogen adsorption−desorption isotherms of support (A) and catalysts (B): (a) Siliceous SBA-15, (b) Al-SBA-15(10), (c) Al-SBA-15(20), (d) Al-SBA-15(30), and (e) Al-SBA-15(40).

Table 1. Textural and Structural Characteristics of Al-SBA-15(x) Supports and Catalysts

sample	Si/Al ratio[a]	S_{BET} ($m^2\ g^{-1}$)[b]	V_P ($cm^3\ g^{-1}$)[c]	D_P (Å)[d]
SBA-15		592	0.84	60.0
Al-SBA-15(10)	14	506	0.78	62.4
Al-SBA-15(20)	25	521	0.79	62.6
Al-SBA-15(30)	42	530	0.81	62.6
Al-SBA-15(40)	58	542	0.82	62.7
Mo−Ni/SBA-15		325	0.62	62.0
Mo−Ni/ Al-SBA-15(10)		314	0.59	63.0
Mo−Ni/ Al-SBA-15(20)		316	0.56	62.9
Mo−Ni/ Al-SBA-15(30)		320	0.48	63.0
Mo−Ni/ Al-SBA-15(40)		330	0.42	63.0

[a]ICP-OES analysis. [b]Surface area by BET method. [c]Pore volume. [d]Pore diameter (BJH method).

mesoporous nature of Al-SBA-15 even after the addition of the metals.

3.3. ^{27}Al MAS NMR Spectroscopy. To analyze the way in which aluminum interacts with the SBA-15 framework, ^{27}Al MAS NMR spectroscopy was performed. For aluminum containing mesoporous supports, the peak at 54 ppm is assigned to aluminum in a tetrahedral environment (structural unit AlO_4) and the peak at 0 ppm is related to octahedral aluminum (structural unit AlO_6).[19] The ^{27}Al MAS NMR spectra of as-synthesized and calcined Al-SBA-15 with various Si/Al (10−40) are shown in Figure 5. Results obviously show the existence of both tetrahedral and octahedral aluminum structural units. The higher intensity of tetrahedral aluminum in the calcined materials indicates that the calcination treatment enhances the incorporation of aluminum into the tetrahedral framework, as reported elsewhere.[20] Therefore, from the ^{27}Al MAS NMR spectral studies, it can be concluded that the incorporation of aluminum by the post synthetic grafting method results in the formation of both the tetrahedral and the octahedral aluminum species.

3.4. Diffuse Reflectance Spectroscopy. Diffuse reflectance spectra of Mo−Ni/Al-SBA-15 catalysts with varying Si/Al ratio were recorded to obtain information about the coordination of nickel and molybdenum oxidic species (Figure 6). The absorbance peaks appearing in the ranges of 220−280, 350, 420 and around 700 nm confirm the presence of molybdenum and nickel species in a different type of environment. In general, the absorption band in the region 200−400 nm is attributed as due to charge transfer transition of O^{2-} to Mo^{6+}. The exact position of this band is reported to depend on the state of molybdenum coordination and aggregation. From the spectra recorded, the absorption band in the range of 200−280 nm and 280−350 nm has been assigned to Mo in the tetrahedral and octahedral environments, respectively. Similarly the broad absorption band in the region 420−700 nm has been attributed to Ni^{2+} species. The absorption edge energy (Eg) calculation in diffuse reflectance spectra gives useful information about the formation of different kinds of species, particularly the size of particles present on the catalysts. The earlier reports[21,22] have shown a blue shift of the molybdenum absorption edge with increase in Al content on the Al-SBA-15 and AlMCM-41 supported Ni−Mo catalysts. A similar phenomenon is also observed in Mo−Ni/Al-SBA-15(10−40) catalysts. Molybdenum edge energy (Eg) calculation was made for Mo−Ni/Al-SBA-15 catalyst (Table 2) and found that the Eg value is high (3.3 eV) in the case of Mo−Ni/Al-SBA-15(10). The value decreased with increasing Si/Al ratio, in the following order Si/Al(10) 3.3 eV > Si/Al(20) 3.2 eV > Si/Al(30) 3.1 eV > Si/Al(40) 3.0 eV > SBA-15 2.8 eV. The lowest Eg value calculated for Mo−Ni/Al-SBA-15 corresponds to support with low Al content (Si/Al ratio = 40) and pure SBA-15. This may be due to the formation of bulk crystalline molybdenum oxide species. There is also evidence for the formation of bulk crystalline molybdenum oxide species in the XRD pattern for these two catalysts (Figure 3).

3.5. TPR. After investigating thoroughly the oxidic form of catalysts by XRD, N_2 adsorption−desorption, DRS, and ICP, it

dx.doi.org/10.1021/cs200385y | ACS Catal. 2012, 2, 127−134

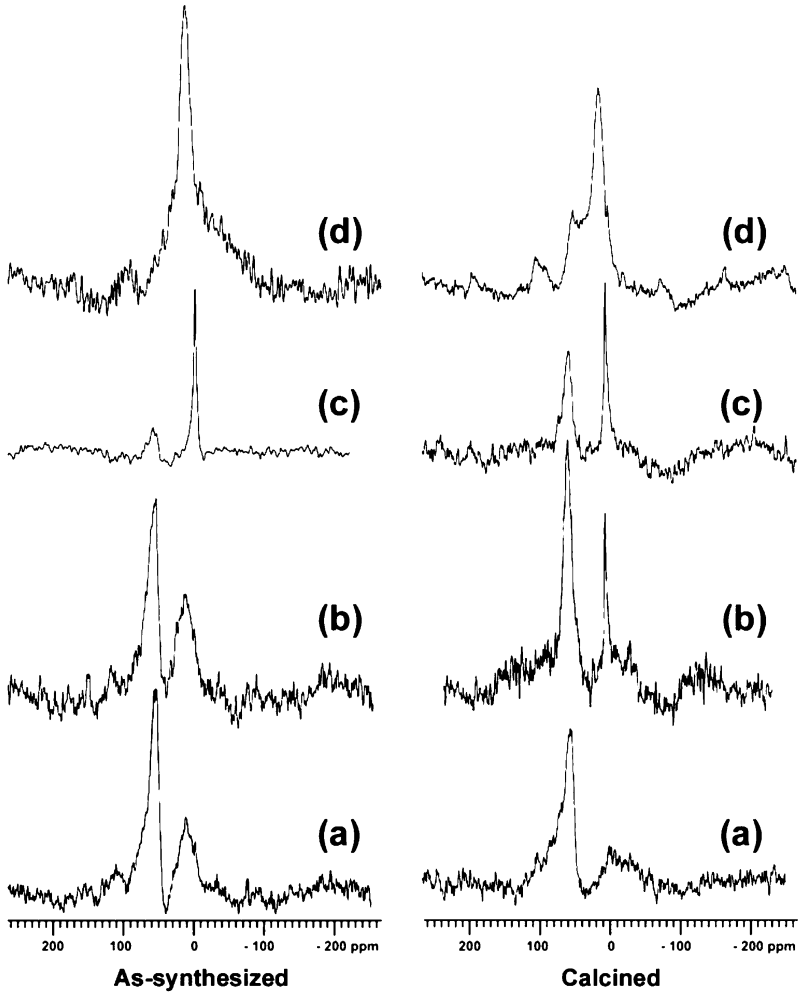

Figure 5. ^{27}Al MAS NMR spectra of as-synthesized and calcined Al-SBA-15 supports: (a) Al-SBA-15(10), (b) Al-SBA-15(20), (c) Al-SBA-15(30), and (d) Al-SBA-15(40).

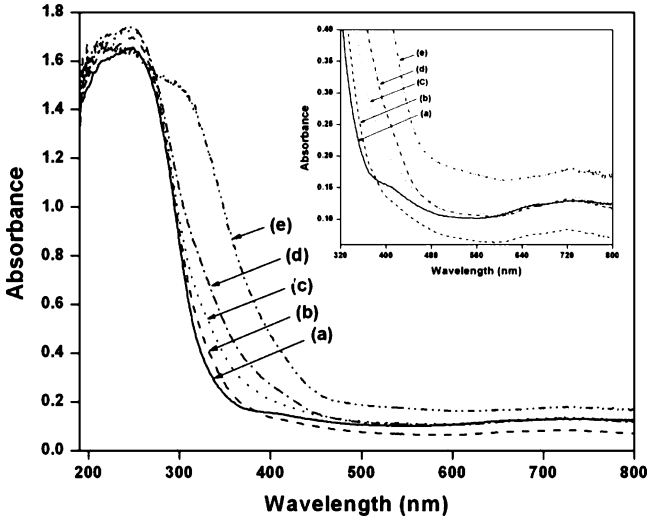

Figure 6. DRS of Mo−Ni/Al-SBA-15 catalysts: (a) Al-SBA-15(10), (b) Al-SBA-15(20), (c) Al-SBA-15(30), (d) Al-SBA-15(40), and (e) SBA-15.

was decided to characterize these catalysts by H_2−TPR, a valuable technique to determine the type and reducibility of the Ni and Mo species present in the oxidic precursors of the catalysts supported over Al-SBA-15.[23] The typical profiles and quantitative data of Mo−Ni/Al-SBA-15 are shown in Figure 7 and Table 2. On examining the TPR profiles, three reduction peaks were traced for Al-SBA-15 and SBA-15 supported Mo−Ni catalysts. The main peak is in the temperature range 430−495 °C; with the other in the range 510−605 °C and a third broad peak is in the high temperature region 625−710 °C. Low temperature peaks in the region of 430−495 °C and 510−605 °C can be ascribed respectively to the first (Mo^{6+} to Mo^{4+}) and second (Mo^{4+} to Mo^{0}) reduction steps of Mo species bound to Al-SBA-15, whereas high temperature peak can be ascribed to the reduction of bulk MoO_3 based on literature.[24] On modification of the support with different Si/Al ratio, a significant shift in the peak temperature was observed. Thus the incorporation of aluminum seems to shift the first reduction peak maximum toward low temperature with concomitant shift in the second reduction peak maximum. In addition, the quantification of TPR peaks shows that there is a variation in hydrogen uptake with Si/Al ratio of Al-SBA-15. Mo−Ni/Al-SBA-15(10) exhibited peak maximum at the lowest temperature with high H_2 uptake, namely, 30 mL/g at STP. The high hydrogen uptake may be accounted for by the formation a large number of easily reducible Mo species distributed uniformly on Al-SBA-15(10). This result suggests that the number and dispersion of active Mo species depend on the Si/Al ratio. This

dx.doi.org/10.1021/cs200385y | ACS Catal. 2012, 2, 127−134

Table 2. Properties and Catalytic Performance of the Catalysts[a]

catalyst	peak maxima (°C) and hydrogen consumption (mL/g STP)			edge energy (Eg) eV[b]	activity × 10^{-4} mol h^{-1} g^{-1}
	1st step reduction (Mo^{6+} to Mo^{4+})	2nd step reduction (Mo^{4+} to Mo^{0})	reduction of bulk MoO_3		
Mo−Ni/ Al-SBA-15(10)	432 (30)	510 (15)	650 (36)	3.3	10.43
Mo−Ni/ Al-SBA-15(20)	445 (18)	522 (27)	643 (43)	3.2	8.51
Mo−Ni/ Al-SBA-15(30)	448 (16)	525 (28)	636 (45)	3.1	7.23
Mo−Ni/ Al-SBA-15(40)	448 (14)	527 (29)	627 (48)	3.0	6.46
Mo−Ni/SBA-15	494 (11)	604 (33)	708 (54)	2.8	5.18

[a]Number in parentheses indicate hydrogen consumption (mL/g STP). [b]Calculated from diffuse reflectance spectra results.

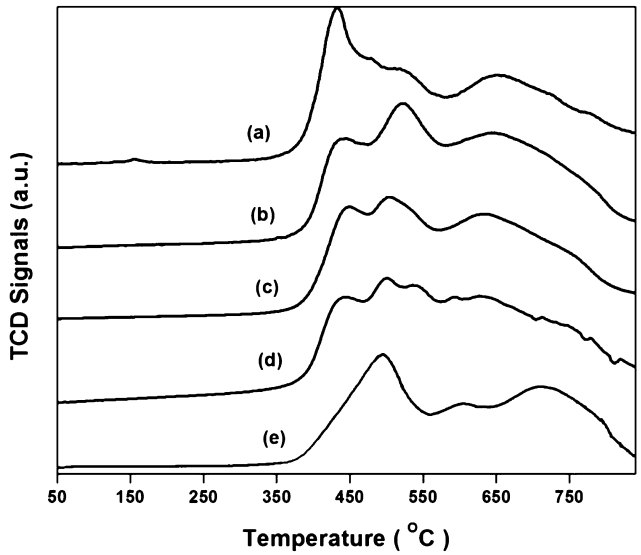

Figure 7. TPR Pattern of Mo−Ni/Al-SBA-15 catalysts: (a) Al-SBA-15(10), (b) Al-SBA-15(20), (c) Al-SBA-15(30), (d) Al-SBA-15(40), and (e) SBA-15.

observation can be supported with XRD and DRS results (Figures 3 and 6). It is to be noted that the TPR profile of Ni−Mo/Al-SBA-15(40) is not well-defined (Figure 7d). The reason for this may be due to a complex interaction between the active species and the support. However in Mo−Ni/SBA-15 catalyst, a relatively large shift in temperature of reduction was noticed toward high temperature. This is attributed to the formation of a large amount of bulk crystalline MoO_3 phase due to poor interaction with siliceous SBA-15 support.

The aforementioned results from XRD, DRS, ICP-OES, and TPR characterization of the Mo−Ni/Al-SBA-15 catalysts clearly show that the proportion of different type of molybdenum species and its dispersion on the support are strongly influenced by Si/Al ratio of Al-SBA-15 for a constant composition of NiO and MoO_3.

4. CATALYTIC ACTIVITY

4.1. Effect of Reaction Temperature. The catalytic activity of sulfided Mo−Ni/Al-SBA-15 (Si/Al = 10−40) catalysts was examined for hydrodenitrogenation of methylcyclohexylamine. The activity of Mo−Ni/Al-SBA-15(10) was measured at various reaction temperatures (320−450 °C) in the presence of ultra high pure grade hydrogen (50 cm^3/min) at atmospheric pressure with 1:30 molar ratio of methylcyclohexylamine to tetralin, and the results are shown in Figure 8. It is seen that the activity of the catalysts increased with the

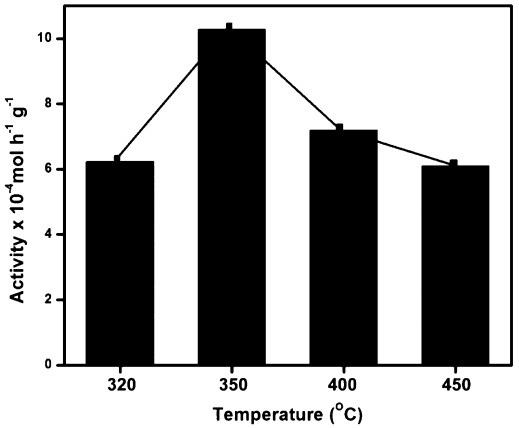

Figure 8. Effect of reaction temperature on hydrodenitrogenation activity of Mo−Ni/Al-SBA-15(10) catalysts: (Reaction Conditions: Reactant: 1:30 mol ratio of MCHA: Tetralin; Reactant Feed: 2 mL/h; Reaction time: 6−8 h).

increase in the reaction temperature up to 350 °C and then decreased beyond 350 °C. The increased activity from 320 to 350 °C shows that this reaction is activation energy demanding. It is to be mentioned that a reaction temperature of 320 °C may not be sufficient to activate the reacting molecule. However, beyond 350 °C, there is high possibility for the molecule to undergo cracking instead of cleavage. Hence, at 350 °C, high activity is observed for the catalyst, Mo−Ni/Al-SBA-15(10).

4.2. Stability with Time. To evaluate the practical applicability and stability of the sulfided Mo−Ni/Al-SBA-15 catalyst with different Si/Al ratio, reaction was carried out at 350 °C for a period of 20 h in the presence of ultra high pure grade hydrogen (50 cm^3 min^{-1}) at atmospheric pressure with 1:30 molar ratio of methylcyclohexylamine and tetralin. The activity profiles presented in Figure 9 show that activity of all the catalysts attains stability after about 3−5 h of exposure to the reactant stream and remains stable up to 20 h under the present experimental condition. The used catalyst was regenerated in a flow of air at 500 °C for 5 h and tested for its reproducibility. It was found that the catalyst was reproducible for many runs. The overall behavior of the catalyst after regeneration shows that catalyst possesses an acceptable level of stability under the present experimental conditions. However, in the case of AlMCM-41 supported

dx.doi.org/10.1021/cs200385y | ACS Catal. 2012, 2, 127−134

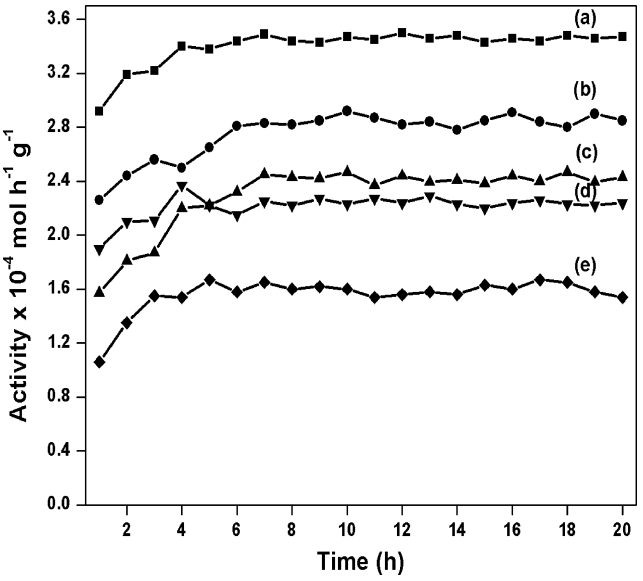

Figure 9. Effect of time on stream and hydrodenitrogenation activity of Mo−Ni/Al-SBA-15 catalysts: (a) Al-SBA-15(10), (b) Al-SBA-15(20), (c) Al-SBA-15(30), (d) Al-SBA-15(40), and (e) SBA-15. (Reaction Conditions: Reaction temperature: 350 °C; Reactant: 1:30 mol ratio of MCHA:Tetralin; Reactant Feed: 2 mL/h; Reaction time: 1−20 h).

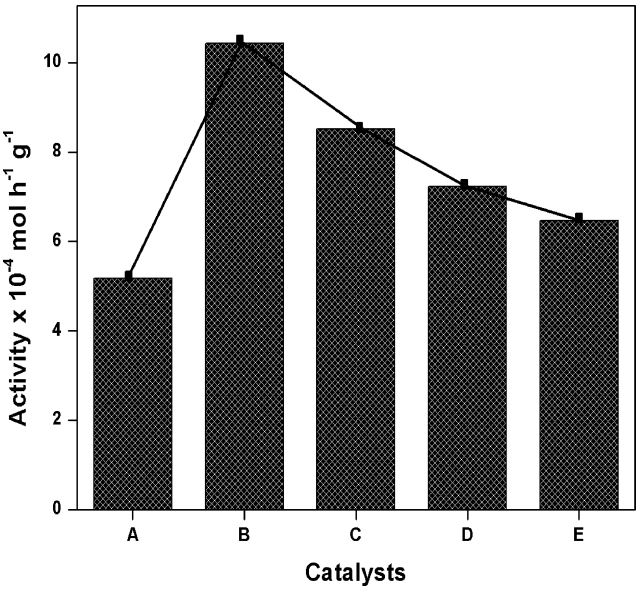

Figure 10. Effect of Si/Al ratio and HDN activity of Mo−Ni/Al-SBA-15 catalysts: (A) SBA-15, (B) Al-SBA-15(10), (C) Al-SBA-15(20), (D) Al-SBA-15(30), and (E) Al-SBA-15(40). (Reaction Condition: Reaction temperature: 350 °C; Reactant: 1:30 mol ratio of MCHA; Tetralin; Reactant Feed: 2 mL/h; Reaction time: 6−8 h).

catalysts the authors[25] reported totally a different trend, namely, a decrease in activity beyond 4 h of reaction time on stream. This study represents the uniqueness of Al-SBA-15 compared to AlMCM-41 supported Mo−Ni catalyst. From the time on stream study, it is concluded that under the laboratory condition Mo−Ni/Al-SBA-15 catalysts have long time durability and stability toward hydrodenitrogenation of the methylcyclohexylamine reaction. The increased thermal stability may be due to its higher wall thickness of the SBA-15 type materials.

4.3. Hydrodenitrogenation Activity as a Function of the Si/Al Ratio. The activities of sulfided Mo−Ni/Al-SBA-15 catalysts with varying Si/Al value (10, 20, 30, and 40) were measured under the experimental conditions described in section 4.2 and the results are presented in Figure 10. A direct trend in the catalytic activity of Mo−Ni catalysts was observed with increase in aluminum content. Among all the catalysts, Mo−Ni/Al-SBA-15(10) rich in aluminum exhibited highest catalytic activity, whereas Mo−Ni/SBA-15 catalyst shows lowest activity. The fine dispersion of Mo species over Al-SBA-15(10) is evident from the absence of peaks corresponding to MoO_3 in XRD pattern and from edge energy values calculated from DRS results (Table 2). It can be concluded that the framework aluminum may help to disperse finely the active and promoter metals which enhances the catalytic performance. A correlation table is presented with hydrogen uptake calculated from quantification of TPR signals, edge energy values calculated from diffused reflectance spectra of oxidic catalysts and catalytic activity of Mo−Ni catalyst supported on Al-SBA-15 with varying Si/Al ratio (Table 2). The results on oxidic form of the catalysts can be extended for interpretation of the activity of the sulfided catalysts. The HDN activity of the catalyst is strongly dependent on the amount and nature of active molybdenum species and hence their dispersion on support. The activity of Mo−Ni catalysts varied systematically with the Si/Al ratio of the Al-SBA-15 support for hydrodenitrogenation.

Further, the acidity of supports can be related to Si/Al ratio values. Support with low Si/Al value has been reported to have high acidity compared with the high Si/Al values.[26] Hence, the activity of the catalysts with varying Si/Al ratio value can be interpreted in terms of surface acidity. Also from the ^{27}Al MAS NMR results it can be seen that the catalyst with low Si/Al ratio has a large number of tetrahedral aluminum in the framework, which are responsible for creating Brønsted acidic sites on the support. The denitrogenation pathway of methylcyclohexylamine mainly occurs via β-elimination and is facilitated by the Brønsted acidity.[10,12] These Brønsted acid sites also help to create a fine dispersion of active and promoter metals on the surface and thereby create more active sites. Hence, it is essential to introduce Brønsted acidity by suitably changing the Si/Al ratio value of Al-SBA-15 support for achieving high catalytic activity.

5. CONCLUSIONS

Siliceous SBA-15 was synthesized using triblock co polymer (P123) as a structure directing agent and aluminum containing SBA-15 material with varying silica to aluminum ratio (10−40) synthesized by a post synthetic grafting procedure. Mo−Ni impregnated catalysts were prepared by sequential wet impregnation of 3% NiO followed by 12% MoO_3 on Al-SBA-15 supports. The incorporation of aluminum into the framework position of silica and the nature of aluminum species were confirmed by ^{27}Al MAS NMR spectroscopy. Examination of Mo−Ni catalyst by XRD and DRS techniques indicated the formation of bulk crystalline MoO_3 on the surface of both Al-SBA-15(40) and SBA-15. Analysis of TPR profiles indicated a gradual decrease in reduction temperature and significant variation in the hydrogen consumption for reduction of molybdenum with varying Si/Al ratio of the support. The improved hydrodenitrogenation activity on aluminum incorpo-

dx.doi.org/10.1021/cs200385y | ACS Catal. 2012, 2, 127−134

ration is mainly due to the substitution of aluminum in the framework of silica matrix, and fine dispersion of the active and promoter metals on the surface leading to the formation of active species responsible for hydrodenitrogenation. From the present studies, it can be concluded that the dispersion of molybdenum on the surface of the SBA-15 depends mainly on the amount and nature of incorporated aluminum species on siliceous support. Al-SBA-15 supported Mo−Ni catalyst seemed to be active and stable fora prolonged reaction time under the experimental conditions for hydrodenitrogenation of methylcyclohexylamine.

AUTHOR INFORMATION

Corresponding Author

*E-mail: kshanthiramesh@yahoo.com. Phone: +91-44-22358654. Fax: +91-44-22200660.

Funding

The authors are grateful to the Defence Research and Development Organization (DRDO) and Department of Science and Technology (DST), New Delhi, India, for financial support for this research work.

ACKNOWLEDGMENTS

The authors are thankful to UGC-DRS and DST-FIST for providing instrumentation facility at the Department of Chemistry, Anna University, Chennai, India.

REFERENCES

(1) Somorjai, G. A. *Surface chemistry and catalysis*; Wiley: New York, 1994.
(2) Prins, R.; De Beer, V. H. J.; Somorjai, G. A. *Catal. Rev. Sci. Eng.* **1989**, *31*, 1−41.
(3) Grzechowiak, J. R.; Mrozińska, K.; Masalska, A.; Góralski, J.; Rynkowski, J.; Włodzimierz Tylus, W. *Catal. Today* **2006**, *114*, 272−280.
(4) Wang, A.; Wang, Y.; Kabe, T.; Chen, Y.; Ishihara, A.; Qian, W.; Yao, P. *J. Catal.* **2002**, *210*, 319−327.
(5) Vradman, L.; Landau, M. V.; Herskowitz, M.; Ezersky, V.; Talianker, M.; Nikitenko, S.; Koltypin, Y.; Gedanken, A. *J. Catal.* **2003**, *213*, 163−175.
(6) Sampieri, A.; Pronier, S.; Blanchard, J.; Breysse, M.; Brunet, S.; Fajerwerg, K.; Louis, C.; Pérot, G. *Catal. Today* **2005**, *107−108*, 537−544.
(7) Gutiérrez, O. Y.; Fuentes, G. A.; Salcedo, C.; Klimova, T. *Catal. Today* **2006**, *116*, 485−497.
(8) Sundaramurthy, V.; Eswaramoorthi, I.; Dalai, A. K.; Adjaye, J. *Microporous Mesoporous Mater.* **2008**, *111*, 560−568.
(9) Muthu Kumaran, G.; Garg, S.; Soni, K.; Kumar, K.; Sharma, L. D.; Murali Dhar, G.; Rama Rao, K. S. *Appl. Catal., A* **2006**, *305*, 123−129.
(10) Rota, F.; Prins, R. *J. Mol. Catal. A: Chem* **2000**, *162*, 367−374.
(11) Rota, F.; Prins, R. *J. Catal.* **2001**, *202*, 195−199.
(12) Qu, L.; Prins, R. *J. Catal.* **2002**, *210*, 183−191.
(13) Zhao, D.; Feng, J.; Huo, Q.; Melosh, N.; Fredrickson, G. H.; Chmelka, B. F.; Stucky., G. D. *Science* **1998**, *279*, 548−552.
(14) Baca, M.; de la Rochefoucauld, E.; Ambroise, E.; Krafft, J. M.; Hajjar, R.; Man, P. P.; Carrier, X.; Blanchard, P. *Microporous Mesoporous Mater.* **2008**, *110*, 232−241.
(15) Sardhar Basha, S. J.; Vijayan, P.; Suresh, C.; Santhanaraj, D.; Shanthi, K. *Ind. Eng. Chem. Res.* **2009**, *48*, 2774−2780.
(16) Shanthi, K.; Pillai, C. N.; Kuriacose, J. C. *Appl. Catal., A* **1989**, 241−249.
(17) Olivas, A.; Zepeda., T. A. *Catal. Today* **2009**, *143*, 120−125.
(18) Zeng, S.; Blanchard, J.; Breysse, M.; Shi, Y.; Shu, X.; Nie, H.; Li, D. *Microporous Mesoporous Mater.* **2005**, *85*, 297−304.
(19) Klimova, T.; Lizama, L.; Amezcua, J. C.; Roquero, P.; Terrés, E.; Navarrete, J.; Domínguez, J. M. *Catal. Today* **2004**, *98*, 141−150.
(20) Luan, Z.; Hartmann, M.; Zhao, D.; Zhou, W.; Kevan, L. *Chem. Mater.* **1999**, *11*, 1621−1627.
(21) Klimova, T.; Reyes, J.; Gutiérrez, O.; Lizama, L. *Appl. Catal., A* **2008**, *335*, 159−171.
(22) Klimova, T.; Calderón, M.; Ramírez, J. *Appl. Catal., A* **2003**, *240*, 29−40.
(23) Klimova, T.; Pena, L.; Lizama, L.; Salcedo, C.; Gutiérrez, O. Y. *Ind. Eng. Chem. Res.* **2009**, *48*, 1126−1133.
(24) Salerno, P.; Mendioroz, S.; López, A. *Appl. Catal., A* **2004**, *259*, 17−28.
(25) Sardhar Basha, S. J.; Sasirekha, N. R.; Maheswari, R.; Shanthi, K. *Appl. Catal., A* **2006**, *308*, 91−98.
(26) Muthu Kumaran, G.; Garg, S.; Soni, K.; Kumar, M.; Gupta, J. K.; Sharma, L. D.; Rama Rao, K. S.; Murali Dhar., G. *Microporous Mesoporous Mater.* **2008**, *114*, 103−109.